Defence Science Journal, Vol. 64, No. 6, November 2014, pp. 502-508, DOI : 10.14429/dsj.64.8110

Coefficient of Drag and Trajectory Simulation of 130 mm Supersonic Artillery Shell with Recovery Plug or Fuze

S. Sahoo[*] and M.K. Laha[#]

[*]*Proof and Experimental Establishment, DRDO, Chandipur-756 025, India*
[#]*Department of Aerospace Engineering, Indian Institute of Technology, Kharagpur-721 302, India*
[*]*E-mail: smrutikgp2011@gmail.com*

ABSTRACT

In the present study, the drag variation and trajectory elements estimation of a supersonic projectile having two different nose shapes are made numerically. The study aims at finding the coefficient of drag and shock wave pattern for 130 mm artillery shell fitted with recovery plug or with fuze, when travelling at zero angle of attack in a supersonic flow of air. The coefficient of drag (C_D) obtained from the simulation is used as an input parameter for estimation of trajectory elements. The numerical results, i.e., the coefficient of drag at different Mach numbers and trajectory elements are validated with the data recorded by tracking radar from an experimental firing. Based on numerical results and data recorded in experimental firing, the coefficient of drag in the case of the shell with recovery plug is 2.7 times more than for the shell with fuze. The shock wave in the case of the shell with recovery plug is detached bow shock wave, whereas in the case of a shell with fuze, the shock is attached. The results indicate that the coefficient of drag increases with detached shock wave and an increase in the radius of the shell nose. Good agreements were observed between numerical results and experimental observations.

Keywords: Coefficients of drag, shock wave, artillery shell, recovery plug, fuze, trajectory simulation, range tables

NOMENCLATURE

C_{Do}	Coefficient of drag at zero yaw
C_D	Coefficient of drag
ρ	Air density
S	Projectile reference area
m	Projectile mass
V	Velocity of projectile
V_x, V_y, V_z	X, Y, Z components of velocity
W	Wind velocity
W_x, W_y, W_z	X, Y, Z components of Wind velocity
t	Time
Θ	Elevation

1. INTRODUCTION

Coefficient of drag is an important parameter in external ballistics. A 130 mm artillery shell at 943 m/s muzzle velocity in vacuum covers a maximum range of 90.7 km whereas in the presence of air, its range reduces to 24 km. Therefore, the coefficient of drag plays a vital role in the case of range and depends strongly on the shape of the nose of the projectile. The two different kinds of projectiles considered here are 130 mm shell with recovery plug and 130 mm shell with fuze. At times, when flat-nosed firing plugs are substituted for ogive-shaped fuzes in a sea-based Proof Range, like PXE, to significantly increase the drag force and air resistance, to reduce the range, terminal velocity, and striking energy of the projectile, then these encounter much higher resistance while penetrating into the sea bed at the target area, thus making subsequent recovery process easier and quicker. Recovery of the shells is very much essential for post-firing inspection to dynamically evaluate it for its strength of design. The range tables (RTs) of 130 mm shell with recovery plug is not readily available to estimate the trajectory elements. The impact points are difficult to locate in the absence of range tables. Proper estimation of co-efficient of drag will be helpful in computation of trajectory elements and generation of range tables. Theoretical estimation of suitable range location is also needed for safe deployment of recovery, and observation teams for easy recovery of shells after firing. Therefore, RTs are essential and for the preparation of range tables, coefficient of drag is an important parameter.

Received 22 August 2014, online published 13 November 2014

2. NUMERICAL ESTIMATION OF COEFFICIENT OF DRAG

The objective of the present study is to estimate numerically the coefficient of drag and shock wave pattern at different Mach numbers for both 130 mm supersonic artillery shell with recovery plug and fuze. The yaw was assumed to be zero in both the cases. Analysis was done numerically with the help of software GAMBIT 2.2 and FLUENT 6.3. The estimated C_D was used as an input parameter for simulation of trajectory elements. The numerical results were validated with experimental data recorded by tracking radar. Finally, comparison was made with the estimated C_D of projectiles with two different nose shapes and the trajectory elements were found out for preparation of range tables.

2.1 Projectile

Both the shells, viz., shell with recovery plug and that with fuze have the same calibre, i.e., 130 mm. The lengths of shell with recovery plug and shell with fuze are 625.2 mm and 674.8 mm, respectively. The mass of both types of shells is 33.4 kg. The recovery plug is of blunt truncated conical shape with higher dia 80 mm, lower dia 55 mm, and length 11 mm, whereas the fuze is of ogive shape with maximum dia 33 mm, minimum dia 14 mm and length 110 mm. The projectiles with dimensions are sketched in Figs 1 and Fig 2.

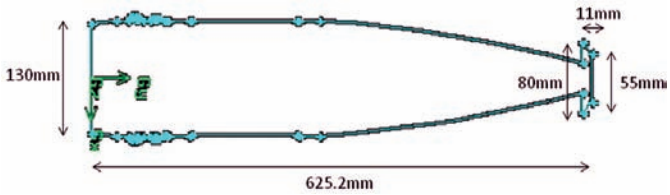

Figure 1. Dimensions of shell with recovery plug.

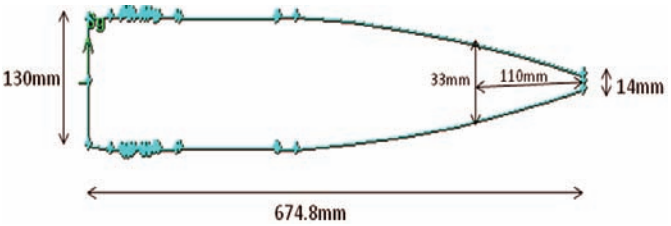

Figure 2. Dimensions of shell with fuze.

2.2 Assumptions

The following assumptions were made for numerical simulation.

- The angle of attack and sideslip are zero.
- The air is an ideal gas.
- The flow is a steady flow.

2.3 Numerical Simulation

The numerical simulations were carried out using software package GAMBIT 2.2 and FLUENT 6.3. The projectile (shell with recovery plug/shell with fuze) was placed at zero angle of attack in a supersonic flow of air. Shell geometry and meshing were made with the help of GAMBIT 2.2. Quad element and map type meshing created for the shell with recovery plug and the shell with fuze are shown in Figs 3 and 4 respectively.

The boundary conditions specified were pressure far-field (top, left side and right side) and axis (bottom), due to axisymmetric shape of the projectile and supersonic nature of flow. The governing equations were solved using a finite volume implicit scheme, that is second-order accurate in space and time. The convective flux terms were discretised using Roe-Finite Difference Scheme (Roe-FDS). Algebraic Multigrid (AMG) method was used for convergence of the implicit density based solver. Shear–stress transport (SST) K-ω turbulence model was used and boundary condition was pressure far-field. The reference values were taken as per the dimensions of projectiles and properties of air. The air was assumed to be an ideal gas and the properties of air such as density, enthalpy, temperature, viscosity and ratio of specific heats were taken as 1.176674 kg/m³, 808504.9 J/kg, 300.0001

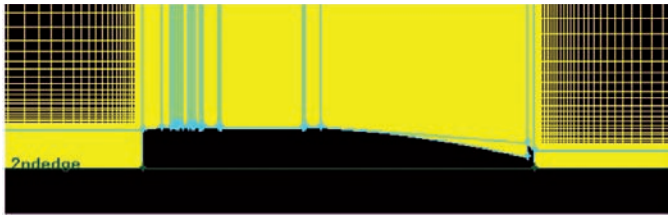

Figure 3. Meshing of shell with recovery plug.

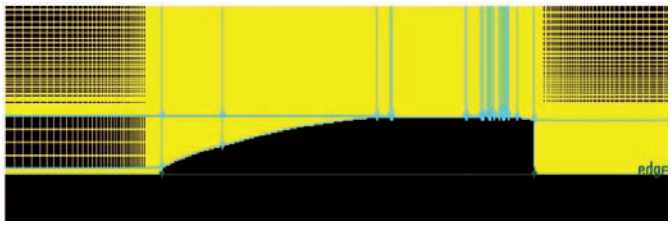

Figure 4. Meshing of shell with fuze.

K, 1.7894 x 10^{-5} kg/m-s, and 1.4, respectively. The simulations were done for two different velocities for each type of shell. For the shell fitted with recovery plug, the velocities were 985.7 m/s and 1006.6 m/s while for the other, these were 996.1 m/s and 1003.1 m/s.

2.4 Simulation Results

The coefficient of drag found at zero yaw for velocities 1006.6 m/s, and 985.7 m/s in case of shell with recovery plug and for velocities 996.1 m/s, and 1003.1 m/s in case of shell with fuze are given in Table 1.

Table 1. Simulated values of C_D at different velocities

Types of shell	Velocity (m/s)	C_D
Shell with recovery plug	1006.6	0.6260
Shell with recovery plug	985.7	0.6429
Shell with fuze	996.1	0.2297
Shell with fuze	1003.1	0.2306

The shock wave pattern observed in case of shell with recovery plug is a detached bow shock wave and in case of shell with fuze, it is an attached oblique shock wave. The pressure contour, density contour, velocity contour and turbulence contour for velocity 1006.6 m/s in case of shell with recovery plug and for velocity 1003.1 m/s in case of shell with fuze are shown in the Figs 5 to 12.

High pressure at nose and low pressure at base of the projectile are observed from Fig. 5. When supersonic air comes in contact with nose of the projectile, it gets a resistance from the nose and slows down, as a result velocity of air decreases and pressure increases (Bernoulli's equation). This high pressure causes fore-body drag at nose. Low (suction) pressure in wake at rear of the projectile causes base drag. This low pressure pulls the projectile rearwards as it moves forward. Both of these drags (fore-body drag and base drag) in combination are known as normal pressure drags. Due to the detached nature of shock wave C_D has a high value of 0.6260 for velocity 1006.6 m/s.

Figure 6 shows a lower pressure at nose and base of the projectile as compared to that having recovery plug, which

reduces normal pressure drag. This is because of the ogive shape of the nose. Due to the attached nature of shock wave as shown in Fig. 6, coefficient of drag found is 0.2306 for velocity 1003.1 m/s.

High density (in the range of 4.27 kg/m³ - 4.53 kg/m³) and low density (in the range of 0.143 kg/m³ - 0.402 kg/m³) are observed (Fig. 7) at nose and base of the projectile respectively. This produces forebody drag and base drag, which help in increasing coefficient of drag.

Low density at the nose and base (0.144 kg/m³ - 0.463 kg/m³) of the projectile are observed from Fig. 8. These factors cause lesser drag as compared to shell with recovery plug.

From Fig. 9 it is noticed that the flow is locally subsonic in the range of 205 m/s - 257 m/s at the nose and base of the projectile. This subsonic (M < 1) range of velocities is due to detached shock wave, as a result of which, high drag is produced.

Figure 10 shows that the flow is supersonic (M > 1) at the nose and subsonic (158 m/s - 210 m/s) at the side face near nose of the projectile. This is due to the formation of attached shock wave.

It is seen from the Fig. 11 that the flow is moderately turbulent at the nose, body, and base of the projectile. The velocity gradient at the surface is much higher for turbulent boundary layer than the laminar boundary layer. This makes it much more difficult to reverse the flow direction, i.e., separate the flow. Therefore turbulent boundary layer decreases base drag, but at the same time, turbulent boundary layer increases surface friction drag. In this case of moderately turbulent nature of flow, the rate of increase of base drag is higher than the rate of decrease of surface friction drag, so the net drag increases.

It is observed from the Fig. 12 that the flow is highly turbulent at the base of the projectile and less turbulent at the body surface. High turbulence at the base of the projectile produces small amount of base drag and low turbulence at the body surface produces small amount of surface friction drag. So, the net drag reduces.

The coefficient of drag at zero yaw (C_{Do}) was determined at various Mach numbers for both plug and fuze cases, the values are given in Table 2 and C_{Do} versus Mach number graphs are plotted in Figs 13 and 14.

It is observed from Fig. 13 that the zero yaw drag coefficient (C_{Do}) for shell with recovery plug increases rapidly with increase Mach number from 0.7 to 1.53 and then decreases. The highest C_{Do} found is 0.7369 at Mach number 1.53.

Similarly Fig. 14 shows that the zero yaw drag coefficient (C_{Do}) for shell with fuze increases rapidly with increase in Mach number from 0.7 to 1.06, and then decreases, but the decrease

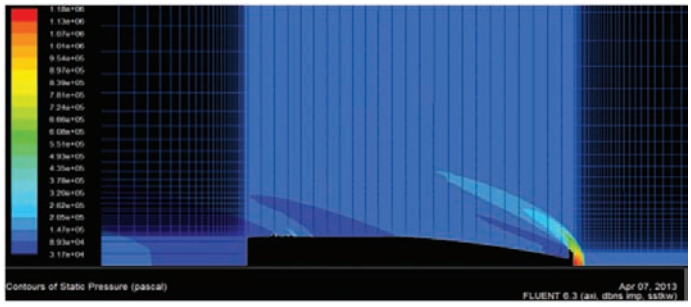

Figure 5. Pressure contour for shell with plug.

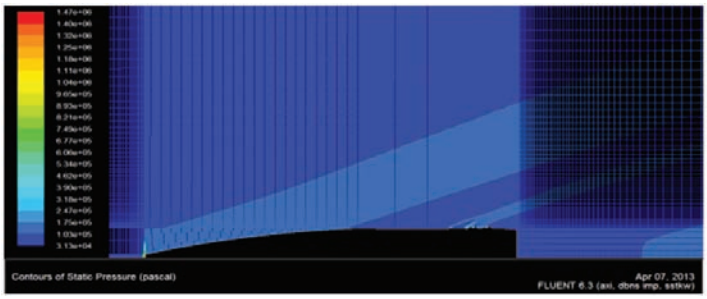

Figure 6. Pressure contour for shell with fuze.

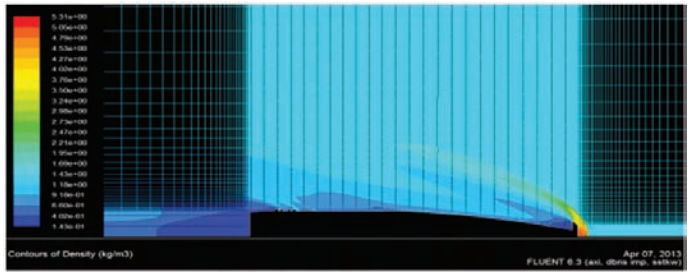

Figure 7. Density contour for shell with plug.

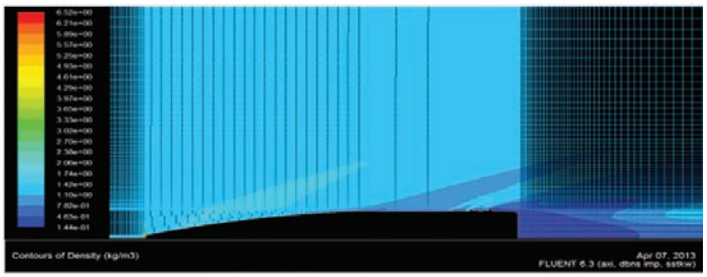

Figure 8. Density contour for shell with fuze.

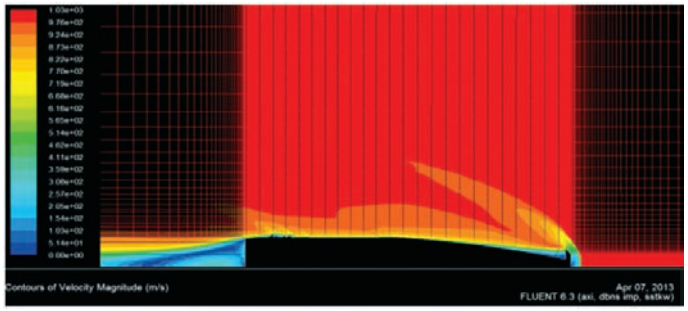

Figure 9. Velocity contour for shell with plug.

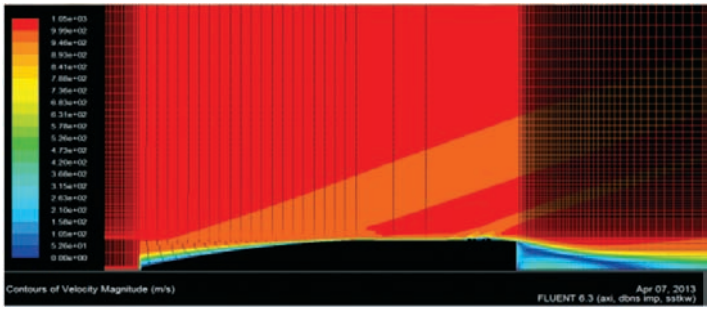

Figure 10. Velocity contour for shell with fuze.

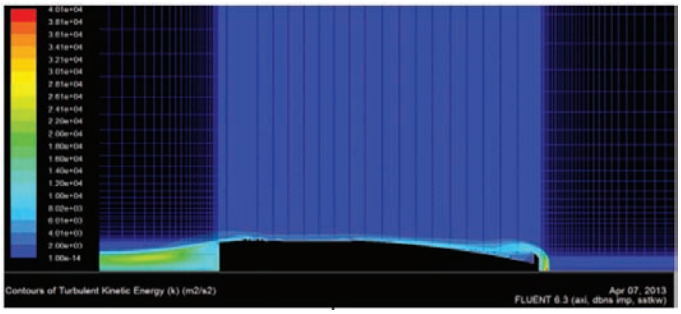

Figure 11. Turbulence contour for shell with plug.

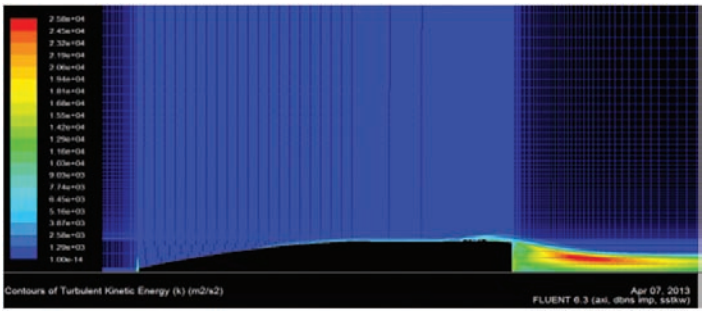

Figure 12. Turbulence contour for shell with fuze.

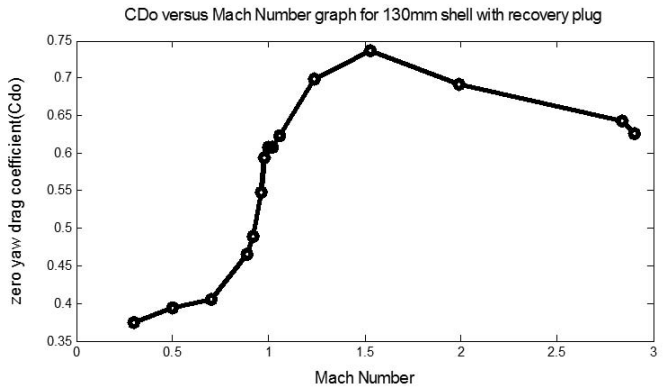

Figure 13. C_{Do} versus Mach number graph of shell with plug.

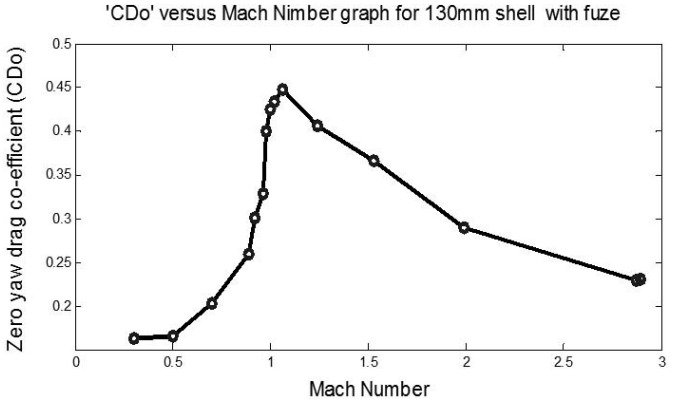

Figure 14. C_{Do} versus Mach number graph of shell with fuze.

Table 2. Drag coefficients at zero yaw (C_{Do}) for various Mach numbers

Shell with recovery plug				Shell with fuze			
Mach No	C_{Do}	Mach No	C_{Do}	Mach No	C_{Do}	Mach No	C_{Do}
0.30	0.3744	1.02	0.6082	0.30	0.1629	1.02	0.4335
0.50	0.3941	1.06	0.6231	0.50	0.1659	1.06	0.4483
0.70	0.4050	1.24	0.6989	0.70	0.2031	1.24	0.4064
0.89	0.4650	1.53	0.7369	0.89	0.2597	1.53	0.3663
0.92	0.4893	1.99	0.6916	0.92	0.3010	1.99	0.2897
0.96	0.5473	2.84	0.6429	0.96	0.3287	2.87	0.2297
0.98	0.5938	2.90	0.6260	0.98	0.4002	2.89	0.2306
1.00	0.6081			1.00	0.4258		

is quite sharp compared to the decrease for shell with recovery plug. The highest C_{Do} found is 0.4483 at Mach number 1.06.

3. SIMULATION OF TRAJECTORY ELEMENTS

The C_{Do} values derived using numerical simulations described in the previous sections were used as input parameters for modelling the trajectory elements. The simulated results were validated with the experimental results provided by tracking radar in dynamic firings.

3.1 Assumptions for Simulation of Trajectory Elements

The following assumptions were made for the simulation of trajectory elements

- The only forces acting on the projectile are gravity force and drag force.
- The projectile is a point mass object.
- The total yaw is small everywhere along the trajectory, so the lift and Magnus force are very small and are neglected.
- The rotation of the earth is ignored.
- The curvature of the earth is ignored.
- The density of air is constant throughout the trajectory.

3.2 Mathematical Model

Trajectory is the path that a moving object follows through space as a function of time. A trajectory can be described mathematically either by the geometry of the path, or as the position of the object over time. If a point mass projectile is projected with some initial velocity under the influence of gravity and air resistance, the coordinate system is shown[1] in Fig. 15.

In this coordinate system (Fig. 15), gun muzzle is located at the origin. The X-axis is directed from the gun towards the target. The Y-axis is directed vertically upward, through the launch point. The Z-axis is directed to the right when looking downrange[1].

Considering gravity and drag to be the only forces

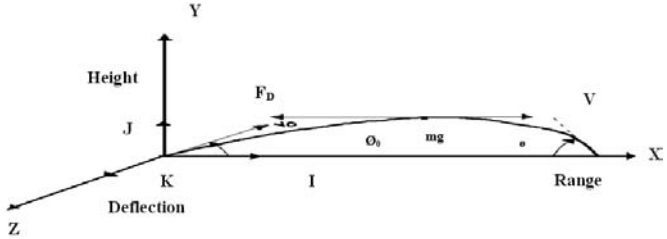

Figure 15. Three-dimensional coordinate system for point mass trajectory.

acting on the projectile, and applying Newton's second law, the equations of motion along three coordinate axes[1] are as follows:

$$\frac{dVx}{dt} = -\frac{\rho SC_D}{2m} VVx \quad (1)$$

$$\frac{dVy}{dt} = -\frac{\rho SC_D}{2m} VVy - g \quad (2)$$

$$\frac{dVz}{dt} = -\frac{\rho SC_D}{2m} VVz \quad (3)$$

In these equations, drag force = (-) $1/2\rho SC_D V^2$, scalar magnitude of velocity vector $V = \sqrt{(V_x^2 + V_y^2 + V_z^2)}$ and acceleration due to gravity (g) = 9.8 m/s^2. Considering tail wind (which, blowing from the gun towards the target is positive Wx, which blowing vertically upward is positive Wy and which blowing from left to right across the line of fire, is positive crosswind, Wz) the equations of motion become[1]:

$$\frac{dVx}{dt} = -\frac{\rho SC_D}{2m}\left\{\sqrt{(Vx-Wx)^2 + (Vy-Wy)^2 + (Vz-Wz)^2}\right\}(Vx-Wx) \quad (4)$$

$$\frac{dVy}{dt} = -\frac{\rho SC_D}{2m}\left\{\sqrt{(Vx-Wx)^2 + (Vy-Wy)^2 + (Vz-Wz)^2}\right\}(Vy-Wy) - g \quad (5)$$

$$\frac{dVz}{dt} = -\frac{\rho SC_D}{2m}\left\{\sqrt{(Vx-Wx)^2 + (Vy-Wy)^2 + (Vz-Wz)^2}\right\}(Vz-Wz) \quad (6)$$

Here scalar magnitude of velocity

$$V = \sqrt{(Vx-Wx)^2 + (Vy-Wy)^2 + (Vz-Wz)^2} \quad (7)$$

Solving Eqns (4), (5), and (7) numerically for simplified 2-D case in Runge Kutta (R-K) fourth order and using initial conditions as initial(muzzle) velocity = $V_{0,}$ initial X-direction velocity $V_x = V_0 \cos \Theta$, initial Y-direction velocity $V_y = V_0 \sin \Theta$, initial coefficient of drag = C_{Do}, initial X-distance(range) = 0, initial Y-distance(height) = 0, initial elevation = Θ_0 and initial time = 0, the elements of the trajectory as terminal V_x, terminal V_y, X-distance(range), Y-distance (height) and time of flight were found out.

3.3 Trajectory Simulation Results

Two cases of initial velocities 996.1 m/s and 1003.1 m/s were studied for the shell fitted with fuze. The C_D values for these velocities are taken from previous simulation results. The other input parameters are the same for these two cases and the values are as follows:

(1) Mass of the projectile 33.4 kg
(2) Dia of projectile 0.13 m
(3) Angle of elevation 7.5°
(4) Wind velocity 0

The Y-distance (height), Y-velocity, X-distance (range), X-velocity values for initial (muzzle) velocities 996.1 m/s and 1003.1 m/s were found wrt time as a result of trajectory simulation and corresponding graphs are shown in (Figs 16 to 21):

The values of the trajectory elements for initial velocities 996.1 m/s and 1003.1 m/s are given in Table 3.

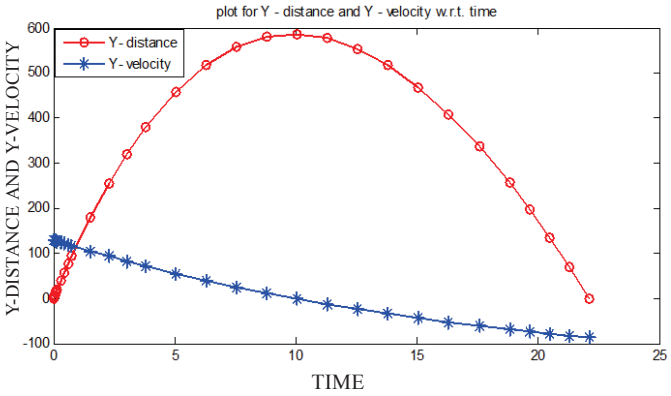

Figure 16. Plot for Y-distance and Y-velocity w.r.t. time for muzzle velocity 996.1 m/s.

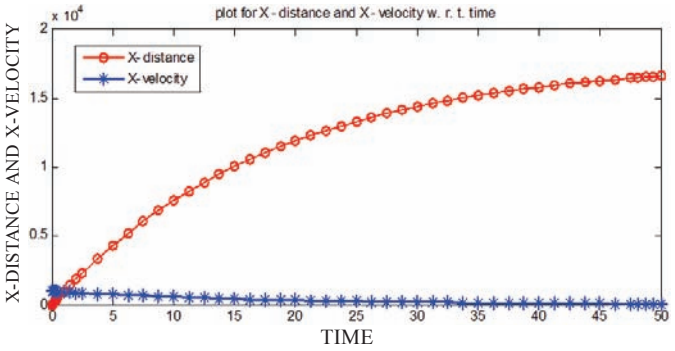

Figure 17. Plot for X-distance and X-velocity wrt time for muzzle velocity 996.1 m/s.

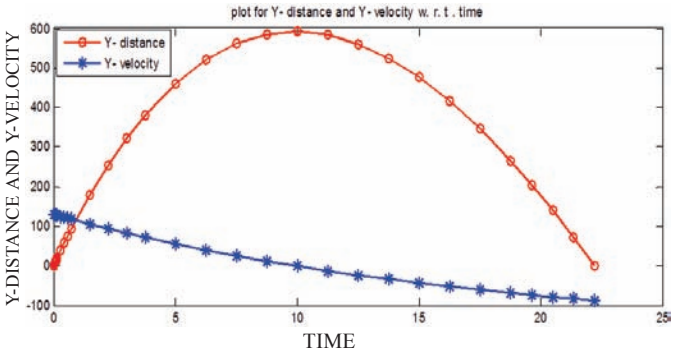

Figure 18. Plot for Y-distance and Y-velocity wrt time for muzzle velocity 1003.1 m/s.

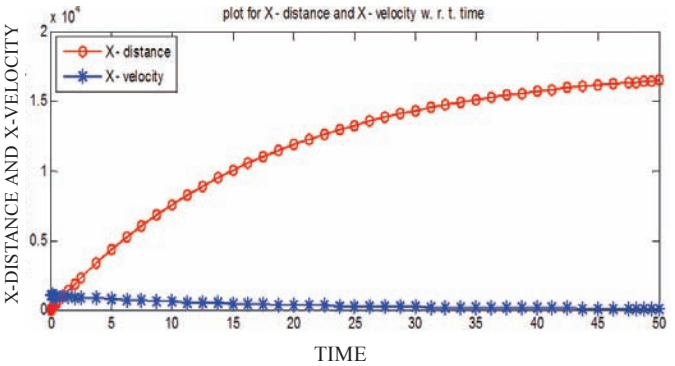

Figure 19. Plot for X-distance and X-velocity wrt time for muzzle velocity 1003.1 m/s.

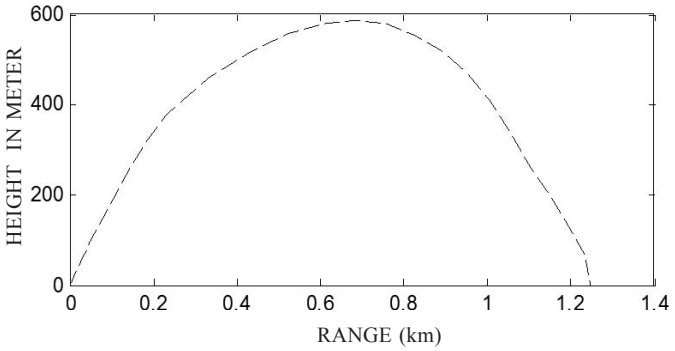

Figure 20. Range versus height graph for muzzle velocity 996.1 m/s.

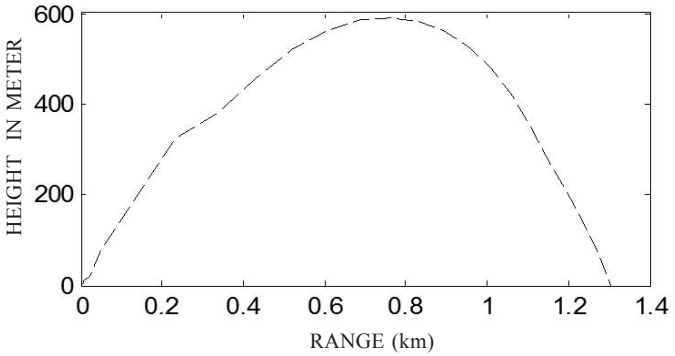

Figure 21. Range versus height graph for muzzle velocity 1003.1/s.

Table 3. Simulated trajectory elements for initial velocities 996.1 m/s and 1003.1 m/s.

For velocity 996.1 m/s		For velocity 1003.1 m/s	
Time of flight (s)	22.09	Time of flight (s)	22.20
Terminal V_y (m/s)	86.69	Terminal V_y (m/s)	86.84
Range (km)	12.48	Range (km)	12.68
Terminal V_x (m/s)	292.0	Terminal V_x (m/s)	276.1

4. EXPERIMENTAL STUDY

Experimental study was undertaken to validate the simulated result by conducting a test firing from 130 mm artillery gun. The sketch of the experimental set up is shown in Fig. 22. A tracking radar was deployed behind the gun, to record the full trajectory of the shells. Two shells fitted with recovery plugs and two shells fitted with fuzes were fired. Shells with recovery plugs were fired at an elevation of 15º and shells with fuze were fired at an elevation of 7.5º.

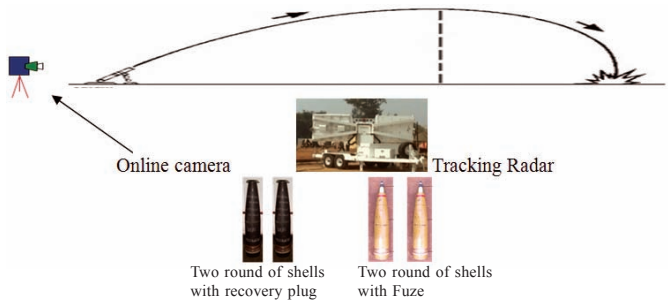

Figure 22. Set up for experimental firing.

The tracking radar recorded the velocities as well as the whole trajectory of the projectiles. From these recordings, the drag coefficient of the projectile was estimated.

4.1 Experimental Results

The C_D values and trajectory elements derived from experimental firings at different velocities are given in Tables 4 and 5.

5. VALIDATION OF SIMULATED RESULTS

A comparison of C_D found from simulated and experimental results is given in Table 6. The error found in case of shell with recovery plug is less than 5.5 per cent and the error found in case of shell with fuze is less than 26 per cent. The error found for shell with fuze is more as compared to shell with plug. This is because of the dimensions of the fuze which were used for simulation and experiment were different. The actual dimensions of the fuze, used at the time of experimental firing were not available. A comparison of trajectory elements found from simulated and experimental results are given in Table 7.

The errors found in case of range and time of flight are less than 6.6 per cent and 0.7 per cent, respectively.

Table 4. Experimental results for C_D at different velocities

Types of shell	Velocity (m/s)	C_D
Shell with recovery plug	1006.6	0.66
Shell with recovery plug	985.7	0.61
Shell with fuze	996.1	0.31
Shell with fuze	1003.1	0.28

Table 5. Experimental results for trajectory elements at different velocities

Initial velocity of 996.1 m/s	Range (km)	13.36
	Time of flight (s)	22.20
Initial velocity of 1003.1 m/s	Range (km)	13.51
	Time of flight (s)	22.05

Table 6. Comparison of numerical C_D with measured values

	Simulated results		Experimental results		Error (%)
	Velocity (m/s)	C_D	Velocity (m/s)	C_D	
Shell with recovery plug	1006.6	0.6260	1006.6	0.66	5.15
	985.7	0.6429	985.7	0.61	5.39
Shell with fuze	996.1	0.2297	996.1	0.31	25.90
	1003.1	0.2306	1003.1	0.28	17.64

Table 7. Comparison of numerical values (trajectory elements) with measured values.

Velocity (m/s)		Simulated results	Experimental results	Error (%)
996.1	Range (km)	12.48	13.36	6.57
	Time of flight (s)	22.09	22.20	0.49
1003.1	Range (km)	12.68	13.51	6.16
	Time of flight (s)	22.20	22.05	0.68

6. CONCLUSION

This simulation can be used for finding zero yaw coefficients of drag and trajectory elements at different Mach numbers for shell with recovery plug or with a fuze. Based on the numerical and experimental results, the coefficient of drag found in case of shell with recovery plug is 2.7 times greater than that of shell with fuze. The shock wave in case of shell with recovery plug is detached bow shock wave, whereas in case of a shell with fuze, it is attached oblique shock wave. The bow shock is due to the blunt shape of recovery plug. Due to the blunt shape, drags like surface friction drag, fore body drag, and base drag are more in case of shell with recovery plug than for shell with fuze. The results indicate that the coefficient of drag increases with detached shock wave and an increase in the radius of the shell nose. The trajectory elements can be used for preparation of range tables. Good agreements were observed between numerical results and experimental observations.

7. ACKNOWLEDGEMENTS

Authors are thankful to Shri R. Appavuraj, Director, and Shri N Nayak, Associate Director of Proof and Experimental Establishment for their encouragement and technical support.

REFERENCES

1. McCoy, R.L. Modern exterior ballistics. Schiffer Military History, Atglen, PA, 1999.
2. FLUENT 6.3 user guide, © Fluent Inc. September 29, 2006.
3. Zitao, Guo; Zhang, Wei; Xinke, Xiao; Gang, Wei & Peng, Ren. An investigation into horizontal water entry behaviours of projectiles with different nose shapes. *Int. J. Impact Eng.,* 2012, **49**, 43-60. doi:10.1016/j.ijimpeng.2012.04.004
4. Zhang, B.; Liu, H.; Chen, F. & Wang, G. Numerical simulation of flow fields induced by a supersonic projectile moving in tubes. *Shock Waves,* 2012, **22**(5), 417-425. doi:10.1007/s00193-012-0389-4
5. Jain, M.K.; Iyengar, S.R.K. & Jain, R.K. Numerical methods for scientific and engineering computation. Wiley Eartern Limited, 1994.
6. Chand, K.K. & Panda, H.S. Mathematical model to simulate the trajectory elements of an artillery projectile proof shot. *Def. Sci. J.*, 2007, **57**(1), 139-148.

CONTRIBUTORS

Ms S. Sahoo is postgraduate in Aerospace Engineering from IIT, Kharagpur and is working in the field of Dynamic Test and Evaluation of Armament Stores at PXE, Chandipur.

Dr M.K. Laha is working in the field of CFD and flight mechanics in the Department of Aerospace Engineering at IIT, Kharagpur.